JOURNAL OF GEOPHYSICAL RESEARCH, VOL. 100, NO. B7, PAGES 9853–9864, JUNE 10, 1995

Long-period regional wave moment tensor inversion for earthquakes in the western United States

Jeroen Ritsema and Thorne Lay

Institute of Tectonics and W. M. Keck Seismological Laboratory, University of California, Santa Cruz

Abstract. Source parameters of moderate to large size ($M_W > 4.5$) earthquakes in the western United States from 1992 to 1994 are determined by point source moment tensor inversion of complete long-period ($T > 35$-50 s) ground motions recorded at regional distances (1°-12°). Stable long-period signals are obtained by low-pass filtering records from the very broadband seismometers recently deployed in several networks in the western United States. These signals are dominated by fundamental mode Rayleigh and Love waves, which have very simple waveforms due to the limited dispersion on the short paths to regional stations. Since long-period motions are relatively insensitive to the attenuation model and crustal structure used in the inversion, they provide robust constraints on the seismic moment and faulting geometry as long as adequate azimuthal coverage is available. Comparisons of solutions for 21 events with results of other regional and teleseismic wave inversions are made to assess the model dependence and uncertainties of our regional centroid moment tensor (RCMT) solutions. RCMT inversion has limited source depth resolution for shallow crustal events, but the focal mechanism and seismic moment determinations prove quite stable over a range of source depths in the crust, as well as over a range of crustal propagation models. Simultaneous waveform inversion of shorter-period body wave signals can improve the source depth resolution. By applying path corrections for heterogeneous crustal structure, shorter-period surface wave energy can also be inverted, allowing the methodology to be extended to lower-magnitude regional events as well. The RCMT procedure requires minimal signal processing, only a sparse broadband network, and a simple laterally homogeneous propagation model; thus it can readily be automated and applied in near real time to events in the magnitude range from 4.5 to 7.5 distributed over an area as large as the western United States.

Introduction

Seismologists have developed numerous methodologies for determining earthquake faulting parameters using seismic recordings at teleseismic (30°-90°) distances [e.g., *Langston and Helmberger*, 1975; *Kanamori and Stewart*, 1976; *Dziewonski et al.*, 1981; *Romanowicz*, 1982; *Sipkin*, 1982; *Ruff and Kanamori*, 1983; *Nabelek*, 1984; *Zhang and Kanamori*, 1988; *Ekström*, 1989; *Kikuchi and Kanamori*, 1991], as well as at very close in distances (< 1°) when strong motion recordings are available [e.g., *Hartzell and Heaton*, 1983; *Beroza and Spudich*, 1988; *Wald et al.*, 1991]. Until recently, relatively little attention has been paid to earthquake source analysis using seismic recordings at regional distances (1°-12°), mainly because regional network seismic instruments saturate when the surface waves arrive for moderate size earthquakes at these ranges, and even if low-gain stations are available, the seismograms are dominated by short-period energy that is difficult to model due to complex propagation effects in the crustal waveguide.

The recent deployment of very broadband (VBB), high-dynamic range digital seismic instrumentation in global as well as regional networks is dramatically improving the capabilities of regional waveform analysis. In the western United States (see Figure 1), the Berkeley Digital Seismic Network (BDSN) [*Romanowicz et al.*, 1994], the California Institute of Technology TERRAscope network [*Kanamori et al.*, 1992a], and the Incorporated Research Institutes of Seismology (IRIS) University Network, are now providing a wealth of high-quality on-scale broadband ground motion recordings that can be used to improve regional wave propagation models [e.g., *Dreger and Helmberger*, 1990; *Zhao and Helmberger*, 1991; *Helmberger et al.*, 1992] and to systematically determine the faulting parameters of regional earthquakes, many of which are too small to produce useful teleseismic signals. Systematic determination of earthquake faulting parameters is now possible in many other regions in the world, such as Japan [e.g., *Nakanishi et al.*, 1991], the Mediterranean [*Giardini et al.*, 1993] and Mexico where networks of broadband stations have been deployed.

Focal mechanisms for the moderate size earthquakes throughout the region provide important information about the regional and local tectonics. The availability of on-scale regional waveforms for large and small earthquakes has accelerated the development of numerous methodologies for analyzing the regional signals for earthquake source parameters. Some of the recent developments include inversions of broadband P_{nl} signals [*Wallace and Helmberger*, 1982; *Dreger and Helmberger*, 1991a, b, 1993; *Lay et al.*, 1994a, b], single-station or sparse network inversions of three-component body wavetrains [*Fan and Wallace*, 1991; *Zhao and Helmberger*, 1993], simultaneous broadband body and surface waveform inversions [*Walter*, 1993; *Zhao and Helmberger*, 1994], spectral inversions of short-period surface waves [*Patton and*

Paper number 95JB00238.
0148-0227/95/95JB-00238$05.00

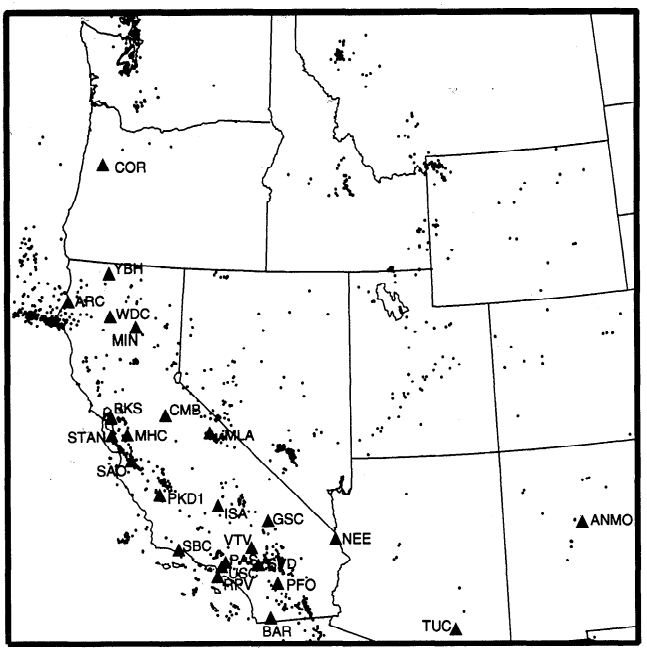

Figure 1. Epicenters of earthquakes with magnitude larger than 4 since 1967 (dots) and location of very broadband instrumentation of the Berkeley Digital Seismic Network (BDSN), TERRAscope and IRIS/University networks (triangles).

Zandt, 1991; *Beck and Patton*, 1991; *Romanowicz et al.*, 1993; *Thio and Kanamori*, 1995], near-field waveform inversion [*Kanamori et al.*, 1990; *Uhrhammer*, 1992], empirical Green's function deconvolutions [e.g., *Kanamori et al.*, 1992b; *Ammon et al.*, 1993], and complete time domain waveform inversions of long-period signals [*Fukushima et al.*, 1989; *Nakanishi et al.*, 1991; *Ritsema and Lay*, 1993; *Giardini et al.*, 1993].

In this paper, we concentrate on waveform inversions using ground motions recorded at regional distances and filtered to retain periods longer than 35-50 s. All of the surface wave energy that eventually reaches teleseismic distances is present in the regional wave field, but with relatively little propagation distortion due to dispersion and attenuation. We adapt the very successful teleseismic centroid moment tensor (CMT) method [*Dziewonski et al.*, 1981; *Kawakatsu*, 1989] to regional distances. Seismic moment determinations tend to be more stable at long periods, and long-period propagation effects are actually simpler at regional distances than at teleseismic distances, unlike for shorter-period body and surface wave signals. The performance of long-period regional waveform inversion is illustrated for a selection of 21 recent earthquakes in the western United States. We tabulate source mechanism solutions, show waveform fits, demonstrate the trade-off of the solutions with velocity models used, and compare with solutions obtained using other methods to determine confidence limits on our long-period regional inversion technique.

Broadband Earthquake Recordings in the Western United States

Figure 1 shows over 2000 widespread epicenters of earthquakes with magnitudes larger than 4 located in the western United States since 1967. These include 250 events with magnitudes larger than 5, giving an average of about nine such earthquakes per year, although recent years have seen heightened seismic activity levels. This seismicity constitutes a significant regional seismic hazard. The locations of the broadband stations used in this study, all of which provide near real-time access to regional recordings, are also shown. The density of stations is high in California, and many of the inversion techniques mentioned above can be used to study nearby earthquakes; however, for other events in the region, broadband stations are sparse and rather distant, complicating analysis of the broadband signals. While additional broadband stations now being deployed will improve the spatial coverage, many regions around the world will only have a few broadband stations, so we have developed a robust method to analyze sparse broadband data sets for regional earthquake source parameters.

A selection of focal mechanisms for earthquakes in 1992-1994 obtained using the method described in this paper is plotted in Figure 2, illustrating the diverse faulting in the western United States. These events have been selected for this analysis based on their spatial distribution and variety of focal mechanisms and source depths; many additional events have been similarly modeled. Notable earthquakes outside California include the Saint George earthquake (event 2) in Utah [*Lay et al.*, 1994b], the Scotts Mill earthquake (event 7) in Oregon [*Nabelek and Xia*, 1995], the Cataract Creek earthquakes (events 8 and 9) in Arizona [*Lay et al.*, 1994a], and the Klamath Falls earthquakes (events 14 and 15) in Oregon [*Dreger et al.*, 1995].

Figure 3a shows a representative three-component VBB recording of the September 2, 1992 Saint George, Utah, earthquake from station ANMO (Albuquerque, New Mexico) at a distance of 675 km. The broadband traces at the top display a complex series of crustal body wave arrivals, followed by large-amplitude Rayleigh and Love waves. Rather than contend with the formidable problem of developing the accurate regional propagation models needed for both broadband body wave modeling and short-period surface wave inversion, we choose to exploit the remarkable bandwidth of the VBB data. We heavily lowpass filter the regional seismograms to extract ground motions at periods longer than 35-50 s. For example,

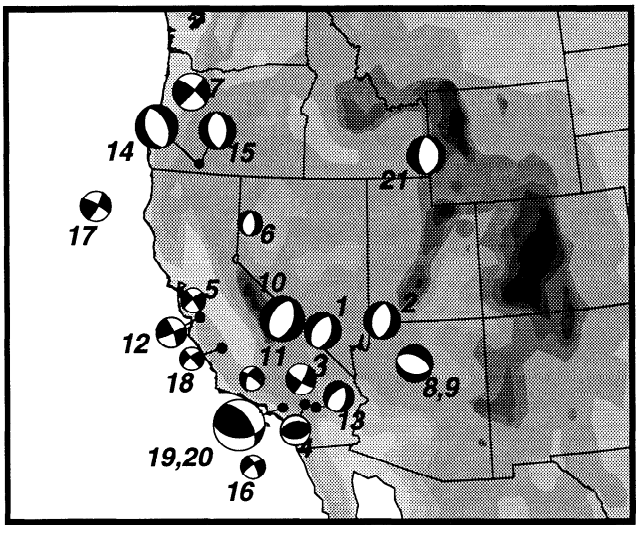

Figure 2. Focal mechanism and epicentral location of earthquakes studied.

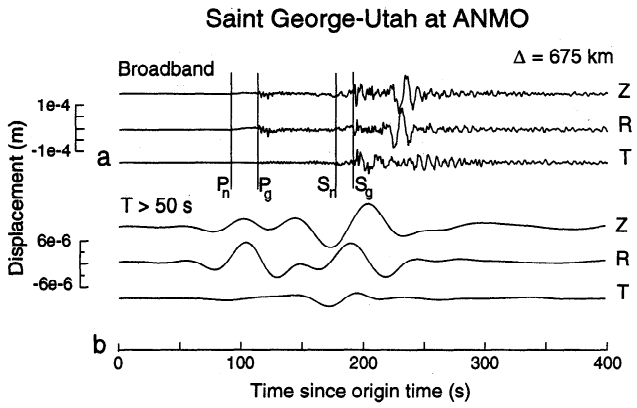

Figure 3. Vertical (Z), radial (R) and transverse (T) component recordings of the Saint George earthquake at ANMO (Albuquerque, New Mexico). (a) broadband displacements and (b) low-pass (T > 50 s) filtered displacements used in regional centroid moment tensor (RCMT) inversion.

the long-period (T > 50 s) energy contained in the regional signals at ANMO is shown in Figure 3b. The ground motions include primarily energy corresponding to the P_{nl} wave and the fundamental mode Rayleigh and Love waves, which are relatively undispersed at this close-in distance. The signal levels are only about 5% of the full broadband waveforms, but the long-period signals excited by this M_W = 5.5 earthquake are recorded at sufficient signal-to-noise ratio to warrant stable waveform inversion. We avoid the windowing procedures required for spectral inversions by inverting the complete long-period waveforms, constructing synthetics with all principle arrivals in the corresponding time window.

Regional Centroid Moment Tensor Method

The regional centroid moment tensor (RCMT) procedure is the regional counterpart to the teleseismic CMT method of *Dziewonski et al.* [1981] as it involves moment tensor inversion of long-period seismic waveforms stabilized by simultaneous relocation of the epicenter and a centroid time shift. The basic theoretical framework for such moment tensor inversions is unchanged from this reference and will not be repeated here. The theoretical seismograms are computed by either normal mode summation or wavenumber integration, and various source velocity models have been considered. Regional long-period (T > 35-50 s) ground motions such as in Figure 3b, are dominated by P_{nl} and fundamental mode surface waves. The overlap of body wave phases and fundamental mode surface waves in the filtered regional waveforms prevents a separate windowing of body waves and surface waves, as in teleseismic CMT inversions, so complete recordings are inverted in RCMT. Three-component recordings are used to exploit the radiation patterns of Rayleigh and Love waves and the relative excitation of long-period surface waves and body waves.

The data going into the inversion are band-pass filtered VBB displacement records of 10-15 min duration from BDSN, TERRAscope, and IRIS University stations (Figure 1) for western United States earthquakes with M_W > 4.5. Earthquakes with M_W > 5 excite seismic periods longer than 50 s well above noise level, so a low-pass filter with this cutoff is usually used, although for events larger than magnitude 7 it is useful to filter more heavily [*Ritsema and Lay,* 1993]. Recordings at distances up to 1500 km span less than seven wavelengths for T > 50 s so that effects of dispersion, attenuation, and focusing are relatively small. Therefore accurate simulation of regional long-period waves can be achieved even with laterally homogeneous velocity models as simple as a layer over a half-space. Smaller-magnitude earthquakes (M_W = 4.5-5.5) can be analyzed using somewhat shorter periods (T > 35 s) and stations within 300 km of the earthquake. From the numerous VBB stations available in the western United States, we select the highest-quality waveform data, eliminating noisy traces and retaining about 4-6 well-distributed stations to ensure stable inversions. Adequate sampling of the Love and Rayleigh wave radiation patterns is critical to obtaining a stable solution. Inclusion of additional stations is straightforward but typically has little effect on the solutions.

RCMT inversions with the preliminary reference earth model (PREM) model [*Dziewonski and Anderson,* 1981] typically yield epicentral relocations of 5-15 km and positive origin time shifts of 8-12 s, with the time shifts being fairly uniform throughout the region. These systematic biases result from the 21.4 km thick crust and 3 km thick water layer in PREM, which is a poor approximation to the shallow structure in the western United States. The origin time shift absorbs most of the phase misalignments caused by using the PREM model, while the epicentral relocations are relatively unimportant in the inversion optimization given the low-frequency signals that are used. Of course, it is not necessary to use PREM, but it is useful to calibrate the RCMT procedure against the teleseismic CMT procedure, which uses PREM for the normal mode excitation.

Figure 4 demonstrates the sensitivity of the RCMT inversion to source location for two earthquakes. The major double couple of the moment tensor solution and the corresponding variance reduction are shown at 25 locations on a 0.1° grid centered on the epicenter reported by the National Earthquake Information Center (NEIC). The origin time is allowed to vary in the inversions, but the epicentral location is held fixed at each grid position. For the Saint George, Utah, event the data were low-pass filtered at T > 50 s, and the optimum epicentral location (dark mechanism) is 0.1° south of the NEIC epicenter. However, the variance reduction improvement is minor, and the focal mechanism is nearly identical to that at the NEIC epicenter. In fact, the mechanism is quite stable over the entire grid, including at positions to the northwest which give comparably good variance reduction. For the September 15, 1992, Landers, California, aftershock, analyzed using TERRAscope records filtered at T > 35 s, there is more variation in variance reduction and moment tensor solution, but the optimum location is at the NEIC epicenter. These two examples are representative of the tendency for centroid relocation to be very minor when using close in recordings (Δ < 400 km), while it can be up to 20 km when using more distant recordings and longer periods; in both cases the mechanism is stably resolved. The small phase shifts involved in the centroid relocation are negligible relative to the periods used in the RCMT inversion, so there is not much advantage to optimizing the source location, unless very poor initial locations are all that is available in a given region.

For the applications in this paper, we have simplified the RCMT routine by omitting optimization of epicentral location, based on the stability in Figure 4, but we still

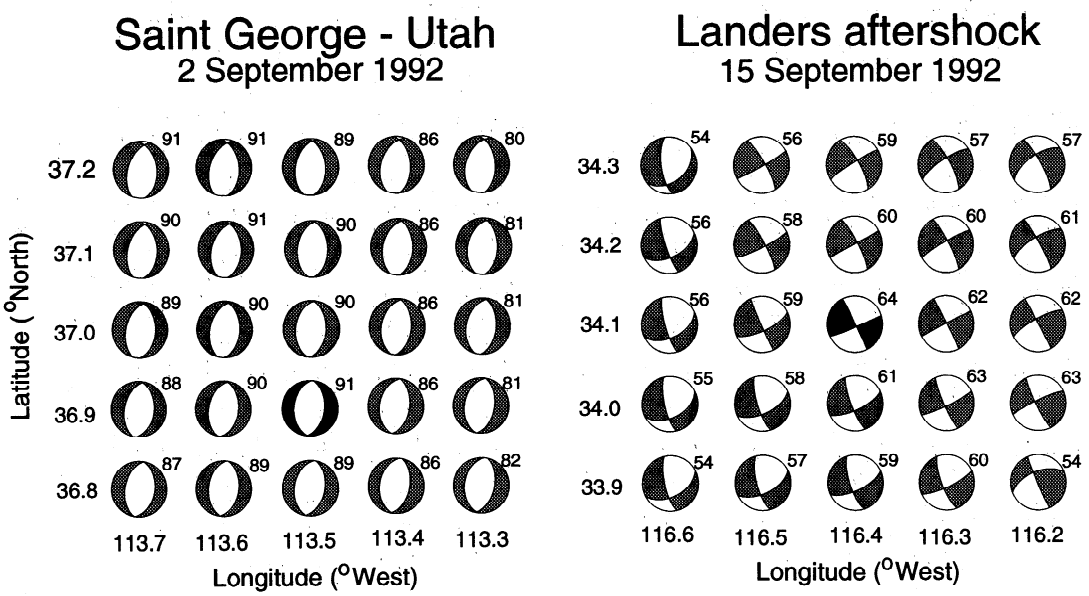

Figure 4. Focal mechanism and variance reduction (printed at the upper right of the focal mechanisms) obtained with RCMT inversion at fixed locations around the National Earthquake Information Center (NEIC) epicenter (center focal mechanism).

optimize the centroid time by cross correlation of waveforms or waveform envelopes. Source depth is estimated by searching over trial depths, as in most inversion methods. In addition, we use a wavenumber integration method to construct the complete regional synthetics, since it is cumbersome to compute complete normal mode data sets for various crustal models. For all of the earthquakes studied we perform RCMT inversions using three models: western United States (WUS), southern California (SC) and PREM (Table 1). Model WUS, developed from phase velocity measurements of surface waves through the western United States (C. Ammon, personal communication), and model SC [*Dreger and Helmberger*, 1993] differ in average crustal velocities by 5% but nonetheless result in very comparable moment tensor solutions and variance reduction. Model PREM, with a much thinner crust than WUS and SC, results in somewhat poorer waveform fits, although the best fitting focal mechanisms are very similar to those obtained with WUS and SC. The effects of the velocity model on the moment tensor estimates can be best understood by considering inversion results for the various models.

Table 1. Velocity Models Used

Depth (km)	*P* velocity (km/s)	*S* Velocity (km/s)	Density [g/cm^3]
	western United States (WUS)		
4.0	4.52	2.61	2.39
32.0	6.21	3.59	2.76
52.0	7.73	4.34	3.22
halfspace	7.64	4.29	3.19
	southern California (SC)		
5.5	5.50	3.18	2.40
16.0	6.30	3.64	2.67
35.0	6.70	3.87	2.80
halfspace	7.80	4.50	3.00
	preliminary reference earth model (PREM)		
12.0	5.80	3.20	2.60
21.4	6.80	3.90	2.90
37.0	8.11	4.49	3.38
57.0	8.10	4.49	3.38
halfspace	8.08	4.47	3.38

Results of RCMT Inversion

Inversions for a selection of 21 earthquakes in 1992-1994 (Table 2) are considered. These events are well distributed throughout the western United States, range in magnitude from 4.5 to 6.6, and have variable mechanisms (Figure 2). Solutions from other regional wave inversion methods and the Harvard teleseismic CMT solutions for the larger earthquakes are available for comparison.

Waveform Fits

The key to the RCMT method is the quality of fits to the simple long-period waveforms. Representative examples of waveform fits to three-component low-pass filtered ($T > 50$ s) ground displacement recordings for events 10 and 21 are displayed in Figure 5. The solid traces are observed waveforms, and the dotted traces are computed for the best fitting source mechanism and source depth, which are indicated below the waveforms. The synthetic waveforms, computed for the WUS model, provide an excellent match to the observed waveforms both in amplitude and phase of P_{nl} and the surface wave signals for propagation paths throughout the entire western United States. Overall least-squares waveform variance reductions are 91.7% and 81.0% for events 10 and 21 respectively, which are typical values. The small effects of dispersion and attenuation over the relatively short propagation paths allows for effective modeling of the long-period waveforms using the laterally homogeneous WUS model. Systematic time shifts are removed by the centroid optimization, but for the WUS model these shifts tend to be only a few seconds. For particular paths, shorter-period waveforms are equally well modeled, but for paths along complex structures, such as the Sierra Nevada or the Central Valley in California, there are strong waveform mismatches for periods less than 35-50 s, and time domain inversion using a homogeneous crustal model is not viable.

Table 2. Earthquake Locations and Regional Centroid Moment Tensor Fault Plane Parameters

	Location	Date	Lat (°N)	Lon (°W)	strike (o)	dip (o)	rake (o)	M_o (10x Nm)	M_w	Depth (km)
1	Skull Mountain	June 29, 1992	36.7	116.2	13	49	-105	3.3 17	5.6	10
2	St George	Sep. 9, 1992	37.1	113.5	9	48	-92	2.4 17	5.5	20
3	Big Bear	Nov. 27, 1992	34.3	116.9	29	78	-14	1.0 17	5.3	10
4	Big Bear	Dec. 4, 1992	34.3	116.9	282	46	104	7.3 16	5.2	10
5	Gilroy	Jan. 16, 1993	37.0	121.5	336	88	191	3.8 16	5.0	10
6	Pyramid Lake	Feb. 10, 1993	40.4	119.6	358	56	-106	1.1 16	4.6	10
7	Scotts Mills	Mar. 25, 1993	45.0	122.6	310	75	173	3.4 17	5.6	22
8	Cataract Creek	Apr. 25, 1993	35.6	112.1	285	53	-83	1.6 16	4.7	12
9	Cataract Creek	Apr. 29, 1993	35.6	112.1	300	49	-72	1.0 17	5.3	12
10	Eureka Valley	May 17, 1993	37.2	117.8	37	49	-66	1.4 18	6.0	10
11	Bakersfield	May 28, 1993	35.1	119.1	205	61	7	1.3 16	4.7	22
12	Alum Rock	Aug. 11, 1993	37.3	121.7	325	82	186	1.8 16	4.8	10
13	Landers	Aug. 21, 1993	34.0	116.3	7	48	-122	6.3 15	4.5	10
14	Klamath Falls	Sept. 21, 1993	42.3	122.0	343	46	-83	1.1 18	6.0	8
15	Klamath Falls	Sept. 21, 1993	42.3	122.0	1	46	-83	1.1 18	6.0	8
16	Off-shore Ensenada	Oct. 18, 1993	31.9	118.9	237	75	-17	1.3 16	4.7	5
17	Off-shore Mendocino	Oct. 23, 1993	40.6	126.7	28	78	16	0.8 17	5.2	8
18	Parkfield	Nov. 14, 1993	36.0	120.5	140	90	161	1.7 16	4.8	8
19	Northridge	Jan. 17, 1994	34.0	118.7	92	49	49	1.1 19	6.6	10
20	Northridge	Jan. 17, 1994	34.3	118.7	95	41	40	8.7 17	5.9	6
21	Eastern Idaho	Feb. 3, 1994	42.7	111.1	356	32	-93	4.2 17	5.7	4

Waveform fits for four stations are plotted in Figure 5, but generally more than four stations are used in the inversions. While *Ritsema and Lay* [1993] were quite successful in using as few as three stations, single-station or two-station inversions usually result in poorly resolved fault dip, rake, and seismic moment due to the weak excitation of long-period waves by the moment tensor elements M_{xz} and M_{yz} [*Kanamori and Given*, 1981], especially for strike-slip earthquakes for which the surface wave radiation pattern depends weakly on changes in fault dip. In the western United States, owing to the abundance of VBB seismic stations, it is easy to include many more observations. Use of 4-6 well-distributed stations ensures fault angle uncertainties less than 20°.

Estimates of Seismic Moment and Source Depth

The source depth is estimated by determining the maximum variance reduction for a series of trial depths. In the western United States, source depths are generally limited to the upper crust, but in regions with subduction zones source depth determination will be more critical. Amplitudes of Rayleigh waves at $T > 50$ s vary by approximately 30% for source depth variations of 6 km in the crust, while long-period Love waves and P_{nl} waves are relatively insensitive to source depth. Thus, in addition to constraining the source mechanism, the ratio of Rayleigh to Love waves and the ratio of Rayleigh to P_{nl} waves are the fundamental diagnostics of source depth.

We observe that the RCMT variance reduction varies by less than 10% for source depths throughout the upper crust, which illustrates the well-known difficulty of estimating source depth of crustal earthquakes using long-period waves. Figure 6a shows the RCMT best double-couple focal mechanisms plotted at the corresponding value of variance reduction for a series of trial source depths spanning a 20 km range for four

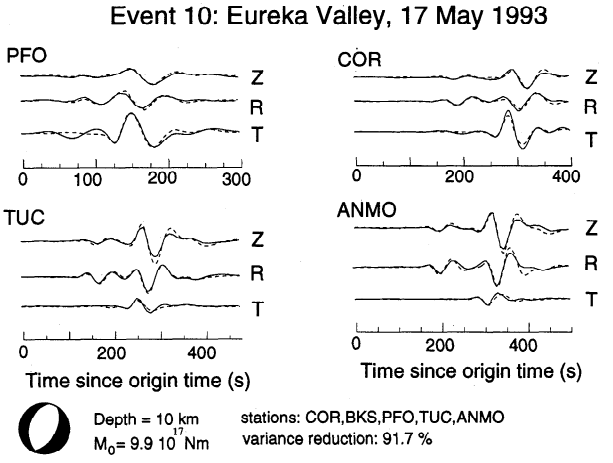

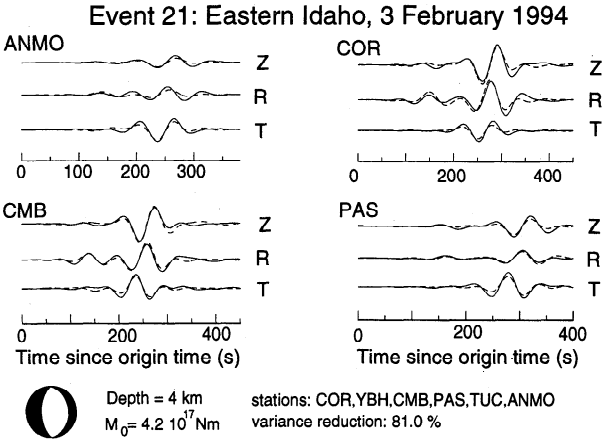

Figure 5. Waveform fit (dotted lines) to observed (solid lines) vertical (Z), radial (R) and transverse (T) component waveforms of events 10 and 21. Waveforms are analyzed at $T >$ 50 s. Best fitting source mechanism is given below the waveform fit.

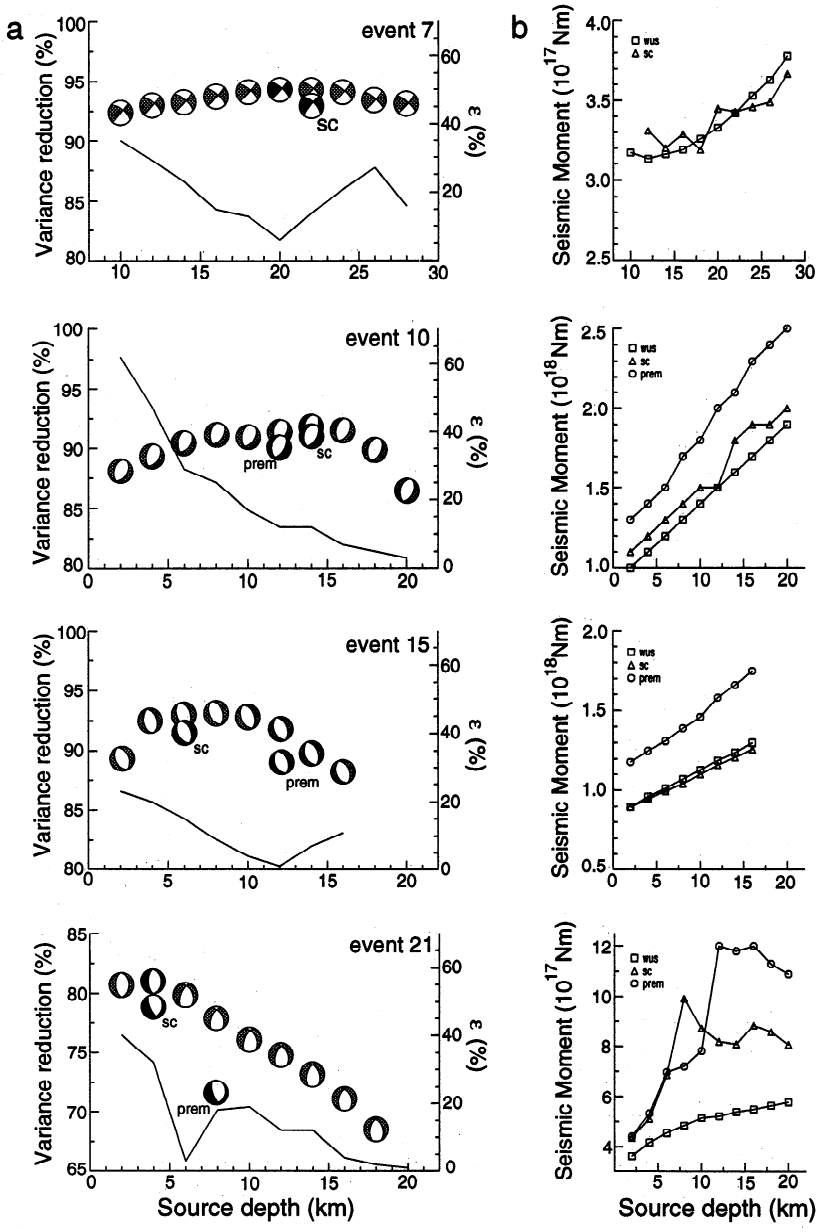

Figure 6. (a) Best double-couple focal mechanism and variance reduction obtained using model WUS for a 20-km source depth interval. The dark focal mechanisms are best fitting solutions for models WUS, SC and PREM. The solid curve represents the percentage of non-double couple component (ε) obtained with moment tensor inversion at various depths. (b) Seismic moment estimate as a function of depth for models WUS, SC, and PREM.

earthquakes, illustrating the limited sensitivity to source depth. In every case there is a maximum variance reduction which can be used to define a optimal source depth, but the variations in variance reduction are small. We estimate the uncertainty in source depth to be ±5 km, based on misfit variations of approximately 50%. This uncertainty also reflects the scatter in source depths commonly observed. While shallow source depths have limited resolution using the long-period waveforms, the uncertainty in source depth does not have much effect on the RCMT focal mechanism. This is very different than for broadband inversions, which tend to be very sensitive to the source depth. Similar depth curves are found for the different crustal models, although model PREM does not give as much variance reduction, and the best fitting solutions for the different models are quite compatible, as shown in Figure 6a.

The solid curves in Figure 6a indicate the non-double-couple component ε, defined as twice the ratio of the smallest and largest eigenvalues of the moment tensor, obtained at each source depth. Assuming that the earthquakes involve pure double-couple fault motion and that the excitation and propagation models are perfectly known, a minimum in ε in principle coincides with the optimum source depth. We consider ε mainly to detect inversion instability and attribute values of ε less than 20% to noise (instrument or model). The dependence of ε on model errors is complex, but one can choose the moment tensor solution with the smallest ε. For example, for event 21 the maximum variance reduction was

obtained at 4 km depth, but the solution has a non-double-couple component of 38%. The moment tensor solution at a depth of 6 km, which has only slightly smaller variance reduction, has $\varepsilon = 4\%$, so this may be preferable in deriving a double-couple faulting model of the event.

Figure 6b shows the seismic moment estimates as a function of source depth. The moment varies systematically with source depth, inversely proportional to the computed Rayleigh wave amplitudes. This is well illustrated by Figure 7, which demonstrates the Rayleigh wave amplitude variations with source depth relative to the less variable P_{nl} and Love waves. The RCMT source depth uncertainty of 5 km yields a 30% seismic moment uncertainty. Additional uncertainty in seismic moment stems from uncertainty in the velocity model used to calculate the Rayleigh wave excitation. The PREM model gives systematically larger moments than the more realistic SC and WUS models as a result of the difference in surface wave excitation. Inversions using a suite of models similar to WUS but with modified crustal thickness ranging over 4 km and modified crustal velocities (varying up to 7%) give quite uniform variance reduction and similar focal mechanisms, so the details of the crustal model are not very important for the long-period inversions. The fluctuations in seismic moment due to a reasonable uncertainty in the propagation model is only about 10%, which is less than the uncertainty associated with depth. Therefore we estimate that the average uncertainty in RCMT seismic moment estimates is less than 40% for most events in the region.

Comparison With Other Methods

We compare the 21 RCMT moment tensor solutions (method 1) with results obtained by the regional methods of *Romanowicz et al.* [1993], and *Thio and Kanamori* [1995] and the teleseismic Harvard CMT inversions. These methods are in routine use and it is therefore interesting to assess the confidence limits on the source parameter determinations. *Romanowicz et al.* [1993] utilize both time domain body wave inversions (method 2) and spectral domain surface wave inversions (method 3). *Thio and Kanamori* [1995] (method 4) invert fundamental mode surface wave spectra using TERRAscope data with an emphasis on southern California earthquakes. All of these regional methods include short-period (T >15-20 s) signals. Harvard CMT (method 5) solutions are available only for the larger earthquakes in Table 2 and are based on body wave signals with periods longer than 45 s and for the largest events, surface waves with periods longer than 135 s.

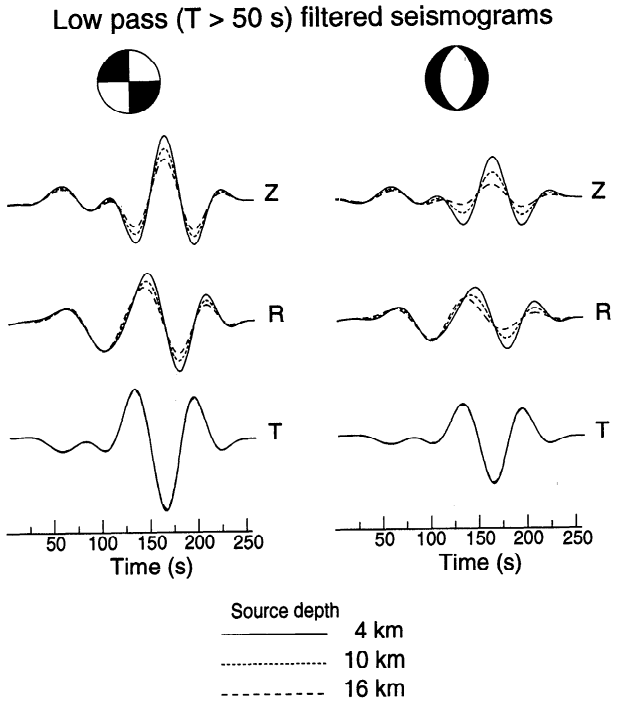

Figure 7. Long-period (T > 50 s) vertical (Z), radial (R) and transverse (T) component waveforms computed for a vertical strike-slip and 45° dip-slip point source at depths of 4, 10, and 16 km at an epicentral distance of 400 km.

Focal Mechanisms

The comparison of major double-couple focal mechanisms from the five methods in Figure 8 is excellent for almost all earthquakes in Table 2. This demonstrates the capabilities of

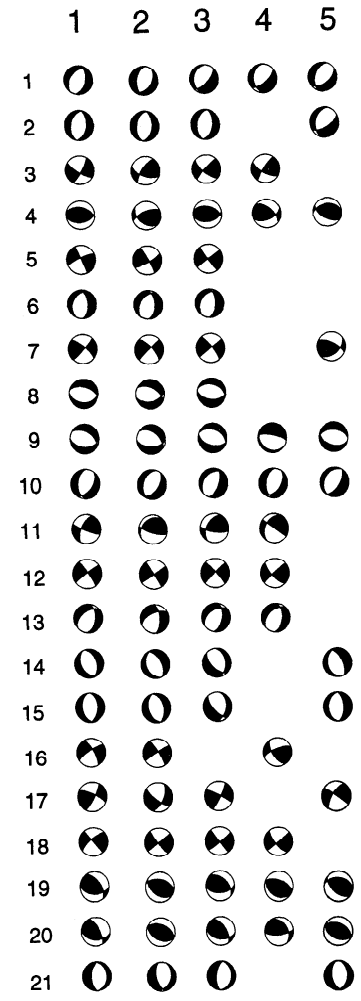

Figure 8. Comparison of best double-couple focal mechanisms obtained with method 1 (RCMT), method 2 (time domain body wave inversion [Romanowicz et al., 1993]), method 3 (spectral surface wave inversion [Romanowicz et al., 1993]), method 4 [Thio and Kanamori, 1995] and method 5 (Harvard CMT).

regional methodologies for reliable determination of overall sense of fault motion, with all of these procedures being easy to apply quickly. The single most significant discrepancy between the five methods is found for event 7 (Scotts Mills, Oregon) for which the Harvard CMT solution is an oblique thrust mechanism, whereas the regional methods resolve predominantly pure vertical strike-slip faulting. Fault angle differences among the five solutions are most significant for the dip and rake angles. Instability of resolving fault dip and rake is evident for each of the four regional methodologies compared here: event 11 (method 1), event 13 (method 2), event 15 (method 3), and event 9 (method 4). This indicates that shorter-period signals still provide limited resolution of the dip-slip moment tensor elements, but generally for all of the methods the dip and rake are resolved within 20° uncertainty.

Seismic Moment and Source Depth

In Figure 9 we compare the source depth and seismic moment estimates for different modeling procedures. Methods 2, 3, and 4 use shorter period signals than RCMT and should in principle have better source depth sensitivity. The scatter in source

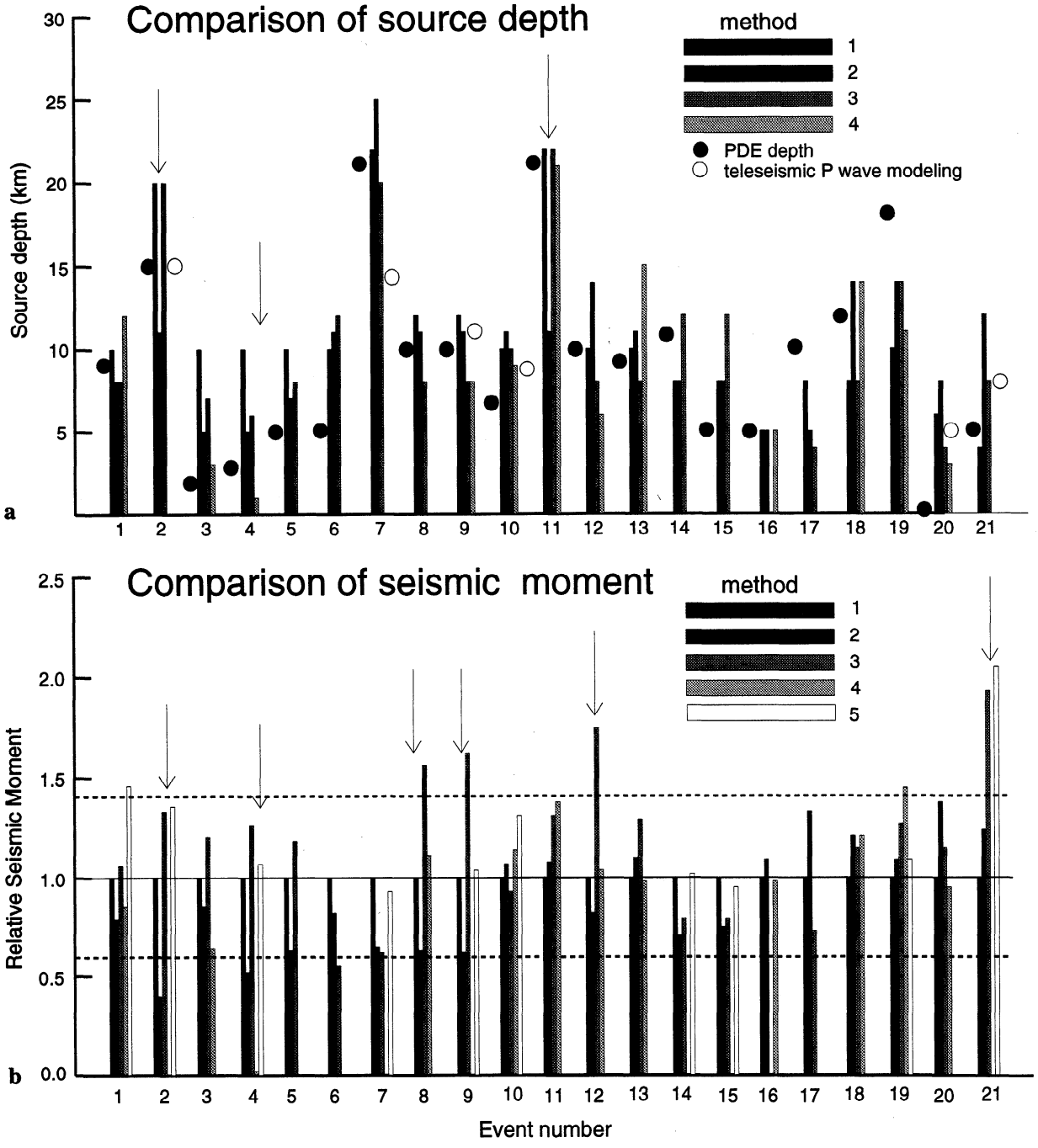

Figure 9. (a) Comparison of source depth obtained with methods 1, 2, 3, 4, 5, Preliminary Determination of Earthquake (PDE) depths, and depths estimated with teleseismic body wave modeling. Arrows highlight significant discrepancies. (b) Comparison of seismic moments relative to RCMT (solid horizontal line). The dotted horizontal lines represents the 40% seismic moment uncertainty of RCMT.

depth estimates obtained with the three shorter-period regional methods is as large as 5 km, which illustrates the complexity of resolving accurate source depth (Figure 9a). Source depth estimates from the preliminary determination of epicenters (PDE) catalogue (solid circles) and our own forward modeling of teleseismic body waves (open circles) supplement the surface wave dominated methods and add to the scatter in source depth estimates. Within this scatter of estimates, it is clear that RCMT source depth estimates are very compatible with depths estimated from presumably higher resolution methods.

Seismic moment estimates from the different methods, normalized by the RCMT seismic moment, scatter over 50% around the RCMT estimates but generally lie within the 40% RCMT uncertainty range (Figure 9b). Several larger discrepancies in seismic moment are highlighted by arrows, with most of these reflecting the coupling of seismic moment estimates with source depth (events 2 and 4), inadequate station coverage (events 8 and 9) [M. Pasyanos and D. Dreger, personal communication], and shallow dip angle (event 21), while other discrepancies (event 12) remain unexplained. Overall the scatter in seismic moment around the RCMT values reflect the 40 % uncertainty we assign to our estimates, so that we are confident our estimates of uncertainty levels are in fact meaningful.

It is straightforward to combine the time domain RCMT inversion method with inversion of P_{nl} waveforms or to expand the frequency content of surface wave signals to corresponding periods less than 35 s in order to improve the resolution of source depth, and hence better estimate the seismic moment. Similar to long-period (T > 15 s) complete waveforms, P_{nl} waveforms at periods larger than 5 s are relatively insensitive to crustal structures and can be adequately modeled with a laterally homogeneous velocity model [*Wallace and Helmberger*, 1982]. Figure 10 demonstrates this for P_{nl} waveform recordings of event 2. Displayed are waveform fits obtained for source depths of 10, 15, and 20 km. The maximum variance reduction (73%) is obtained at a depth of 15 km, intermediate to the depths obtained with other regional methods (Figure 9). The variance reduction over a source depth range of 20 km has a much better defined maximum than obtained using long-period complete waveforms (e.g., Figure 6) and illustrates the value of P_{nl} waveforms in constraining source depth. An inversion procedure in which RCMT inversion precedes a combined inversion of long-period complete waveforms and P_{nl} waveform inversion is a logical extension of the RCMT method to overcome limited source depth resolution and associated uncertainty in seismic moment. A similar scheme has proven successful in teleseismic analysis [*Ekström*, 1989].

Including shorter-period signals in the surface waves is another means of achieving better source depth resolution but accurate and path dependent Green functions must be developed. Short-period (T > 20 s) surface waves have been successfully analyzed to quantify numerous western United States earthquakes either in the spectral domain, where it is possible to suppress the influence of model induced phase mismatches [e.g., *Patton and Zandt*, 1991; *Romanowicz et al.*, 1993] or in the time domain [*Romanowicz et al.*, 1993; *Walter*, 1993], generally restricted to epicentral distances shorter than 500 km. The current tomographic phase velocity models of fundamental mode surface waves do not necessarily guarantee that it is possible to accurately model short-period (T > 20 s) surface waves traveling over distances longer than 1000 km for every particular path throughout the western United States. Figure 11a and 11b compare synthetics, computed with model WUS and source parameters given in Table 2 with observed waveforms for events 10 and 21. At T > 50 s (used in RCMT inversion) the phase mismatch is relatively small, and enables stable moment tensor inversion with a minor centroid time shift applied. At T > 20 s the misalignment is a larger fraction of the seismic period and can not be mapped into a centroid shift without affecting the source parameters that are inverted for. It is possible to separately invert body and surface waves and allowing separate alignments being applied to the body

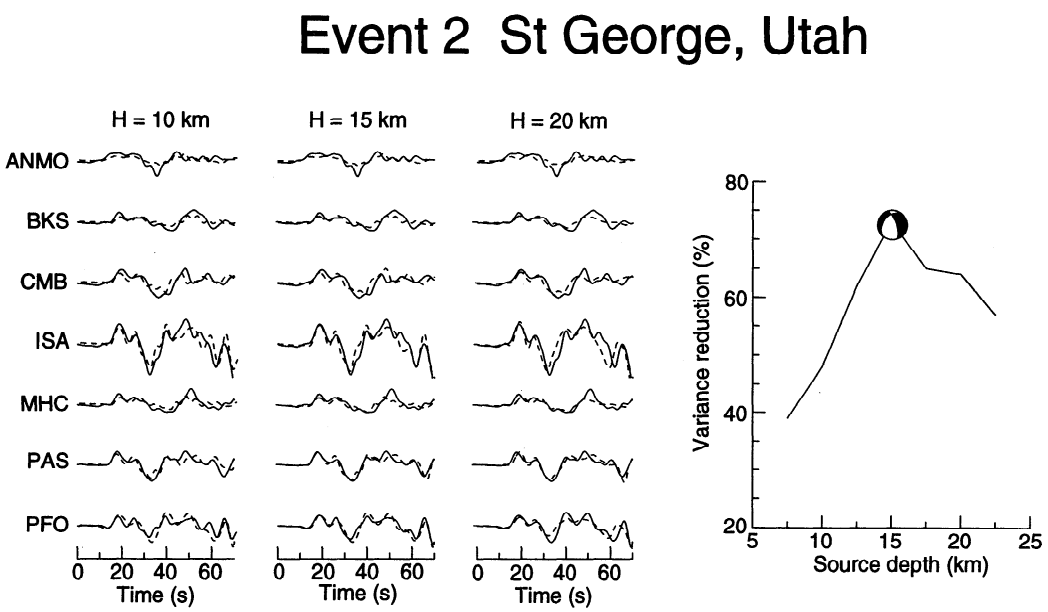

Figure 10. Best fitting synthetic (dotted lines) and recorded (solid) P_{nl} waveforms (T > 5 s) for the Saint George, Utah, earthquake (event 2) obtained at source depths of 10, 15, and 20 km and variance reduction as a function of source depth. Maximum variance reduction (73%) is obtained at a depth of 15 km.

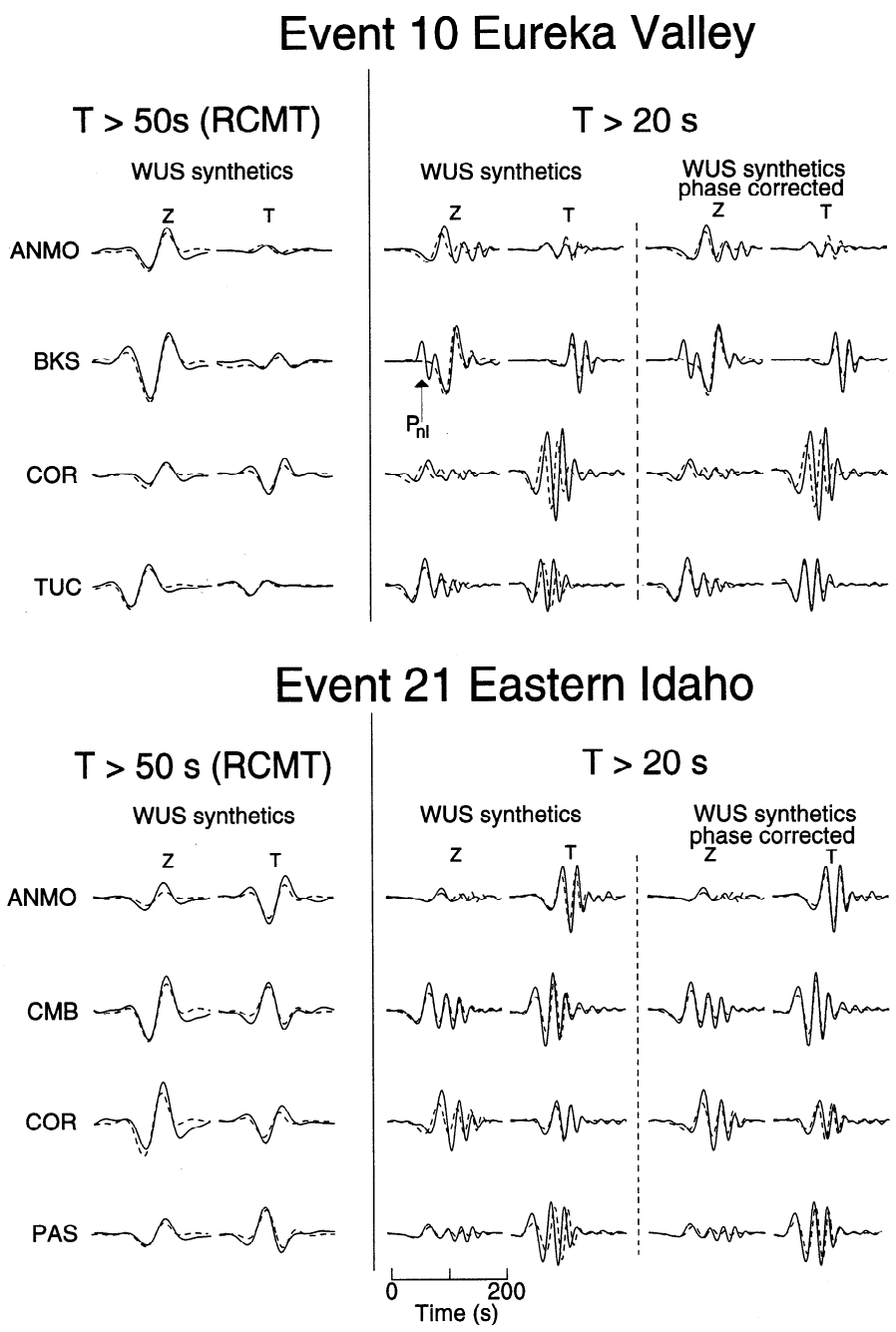

Figure 11. Comparison of observed (solid) and synthetic (dotted) waveforms using model WUS, low-pass filtered at $T > 50$ s (used in the RCMT inversion) and $T > 20$ s. The WUS synthetics in the third column are phase shifted using a frequency dependent phase velocity model determined by C. J. Ammon.

and surface waves trains [*Zhao and Helmberger*, 1994] but using segmented records to infer both source parameters and path corrections involve the risk that a portion of the source phase is mapped into the time shift and vice versa. Ideally, phase corrections are applied using a propagation model obtained with data independent from used in the source inversion. At $T > 20$ s phase corrections based on as recent tomographic model of the western United States [C. Ammon, personal communication] eliminate or reduce waveform misalignments for paths predominantly sampling the Basin and Range structure (event 21 recorded at ANMO, CMB, COR, PAS), however, the Rayleigh and Love waves excited by the Eureka Valley earthquake recorded at COR (Corvalis, Oregon) illustrate a case where the tomographic model fails to account for the delay caused by surface wave propagation along the Sierra Nevada. These mismatches preclude a stable waveform inversion. In those cases where the basic wave shape is well modeled but there is simply a time offset, we suggest an iterative procedure in which the long-period energy is first inverted by the RCMT method, and the solution is used to predict shorter-period signals. If the signal coherence is high, time shifts determined by optimal cross-correlation can be used to align the shorter-period surface waves, and then the inversion is repeated to optimize the source depth. This iterative procedure will reduce the possibility of projecting source phase into the correction terms used for the short-period surface wave signals.

Ultimately higher-resolution tomographic models will become

available, eliminating the need for ad hoc time shifts of the waveforms. Such models will also provide a basis for synthesizing refracted signals, allowing use of stations that now have to be omitted because of poor waveform matches. However, most other regions in the world lack the high density of stations found in the western United States, so inversion strategies such as RCMT, involving robust long-period complete waveform inversion using stations at distances up to 1500 km, seem most viable for systematic quantification of moderate size events.

Discussion and Conclusions

The new very broadband seismic instrumentation in the western United States provides high-quality on-scale regional waveform data that can be used to estimate earthquake faulting parameters for regional earthquakes between magnitudes 3.5 and 7.5. Whereas most regional wave inversion methods use either broadband body waves or surface wave spectra, we have developed a very stable moment tensor inversion method that emphasizes the long-period end of the broadband spectrum. Regional earthquakes with magnitudes larger than 4.5 excite adequate long-period signal (T > 35-50 s) to allow stable time domain waveform inversions given four to six well distributed broadband seismic stations. Long-period waveform inversion has been very successful at teleseismic distances, and the advantages of this approach extend to regional distances as well. Propagation paths to regional stations span no more than seven wavelengths; hence the effects of attenuation and dispersion are small and a laterally homogeneous Earth model suffices for calculating synthetic waveforms. Velocity models with crustal thickness of 28-32 km and reasonable P and S wave velocities result in similar variance reduction, typically between 80% and 90% for events throughout the western United States. Using a standard Earth model like PREM gives smaller variance reduction but still yields a robust focal mechanism. This implies that RCMT type inversion will be readily applicable in regions with poorly known crustal structures.

Source depths are not very well determined using long-period waves, although our depth estimates prove very compatible with those from other regional inversion methods. Uncertainty in source depth has little effect on the determination of focal mechanism for the RCMT method, and for a 12 km range of source depth within the upper crust, seismic moment estimates vary by no more than 30%. Simultaneous inversions of long-period surface waves and short-period (T > 5 s) P_{nl} waves or short-period surface waves with heterogeneous model corrections can increase source depth resolution, reducing the seismic moment uncertainty.

The RCMT method requires only simple signal processing making it very useful for rapid and routine determination of earthquakes of magnitudes larger than 4.5 in a vast seismically active area such as the western United States. With the real-time telemetry technology currently available, obtaining robust estimates of source parameters is principally delayed by the propagation of fundamental mode surface wave to the seismic stations. With rapid data retrieval and data processing, including low-pass filtering and windowing, it is realistic to achieve determination of earthquake faulting process within 15 minutes of the event. Such rapid determination is useful to coordinate post earthquake emergency response activities and deployments of instruments for aftershock studies, and is the first step in the determination of the actual fault plane and slip distribution.

Acknowledgments. Our inversions of regional seismic recordings have been enabled by the open data access policy now prevalent in the seismic community. In particular, we thank broadband station operators of the Caltech TERRAscope, University of California, Berkeley BDSN, and IRIS University networks for rapid access to their seismic data. H. Kawakatsu kindly provided a copy of his CMT inversion program that we adapted for this application. This research is supported by the United States Geological Survey (USGS) Department of the Interior, under USGS award number 1434-94-G2442 to UCSC. The views and conclusions contained in this document are those of the authors and should not be interpreted as necessarily representing the official policies, either expressed or implied, of the United States Government. This is contribution number 264 of the Institute of Tectonics.

References

Ammon, C. J., A. A. Velasco, and T. Lay, Rapid determination of rupture directivity: Application to the 1992 Landers (M_s = 7.4) and Cape Mendocino (M_s = 7.2) California earthquakes, *Geophys. Res. Lett., 20*, 97-100, 1993.

Beck, S. L., and H. J. Patton, Inversion of regional surface-wave spectra for source parameters of aftershocks from the Loma Prieta earthquake, *Bull. Seismol. Soc. Am., 81*, 1726-1736, 1991.

Beroza, G. C., and P. Spudich, Linearized inversion for fault rupture behavior: Application to the 1984 Morgan Hill, California, earthquake, *Bull. Seismol. Soc. Am., 78*, 6275-6296, 1988.

Dreger, D. S., and D. V. Helmberger, Broadband modeling of local earthquakes, *Bull. Seismol. Soc. Am., 80*, 1162-1179, 1990.

Dreger, D. S., and D. V. Helmberger, Source parameters of the Sierra Madre earthquake from regional and local body waves, *Geophys. Res. Lett., 18*, 2015-2018, 1991a.

Dreger, D. S., and D. V. Helmberger, Complex faulting deduced from broadband modeling of the February 28, 1990 Upland earthquake (M_L = 5.2), *Bull. Seismol. Soc. Am., 81*, 1129-1144, 1991b.

Dreger, D. S., and D. V. Helmberger, Determination of source parameters at regional distances with three-component sparse network data, *J. Geophys. Res., 98*, 8107-8125, 1993.

Dreger, D. S., J. Ritsema, and M. Pasyanos, Broadband analysis of the 21 september 1993 Klamath Falls earthquake sequence, *Geophys. Res. Lett.*, in press, 1995.

Dziewonski, A. M., and D. L. Anderson, Preliminary reference Earth model, *Phys. Earth Planet. Inter., 25*, 297-356, 1981.

Dziewonski, A. M., A. T. Chou, and J. H. Woodhouse, Determination of earthquake source parameters from waveform data for studies of global and regional seismicity, *J. Geophys. Res., 86*, 2825-2852, 1981.

Ekström, G. A., A very broadband inversion method for the recovery of earthquake source parameters, *Tectonophysics, 166*, 73-100, 1989.

Fan, G., and T. C. Wallace, The determination of source parameters for small earthquakes from a single, broadband seismic station, *Geophys. Res. Lett., 18*, 1385-1388, 1991.

Fukushima T., D. Suetsugu, I. Nakanishi, and I. Yamada, Moment tensor inversion for near earthquakes using long-period digital seismograms, *J. Phys. Earth, 37*, 1-29, 1989.

Giardini, D., E. Boschi, and B. Palombo, Moment tensor inversion from Mednet data, (2) Regional earthquakes of the Mediterranean, *Geophys. Res. Lett., 20*, 273-276, 1993.

Hartzell, S. H., and T. H. Heaton, Inversion of strong ground motion and teleseismic waveform data for the fault rupture history of the 1979 Imperial Valley, California, earthquake, *Bull. Seismol. Soc. Am., 73*, 1553-1583, 1983.

Helmberger, D. V., R. Stead, P. Ho-Liu, and D. S. Dreger, Broadband modeling of regional seismograms; Imperial Valley to Pasadena, *Geophys. J. Int., 110*, 42-54, 1992.

Kanamori, H., and G. S. Stewart, Mode of the strain release along the Gibbs Fracture Zone, Mid-Atlantic ridge, *Phys. Earth Planet. Inter., 11*, 312-332, 1976.

Kanamori, H., and J. W. Given, Use of long-period surface waves for rapid determination of earthquake source parameters, *Phys. Earth Planet. Inter., 27*, 8-31, 1981.

Kanamori, H., J. Mori and T. H. Heaton, The 3 December 1988, Pasadena earthquake (M_L =4.9) recorded with the very broadband system in Pasadena, *Bull. Seismol. Soc. Am., 80*, 483-487, 1990.

Kanamori, H., E. Hauksson, and T. Heaton, TERRAscope, *Eos Trans. AGU, 73*, 371, 1992a.

Kanamori, H., H.-K. Thio, D. Dreger, and E. Hauksson, Initial investigation of the Landers, California, earthquake of 28 June 1992 using TERRAscope, *Geophys. Res. Lett., 19*, 2267-2270, 1992b.

Kawakatsu, H., Centroid single force inversion of seismic waves generated by landslides, *J. Geophys. Res., 94*, 12366-12374, 1989.

Kikuchi, M., and H. Kanamori, Inversion of complex body waves - III, *Bull. Seismol. Soc. Am., 81*, 2335-2350, 1991.

Langston, C. A., and D. V. Helmberger, A procedure for modeling shallow dislocation sources, *Geophys. J. R. Astron. Soc., 42*, 117-130, 1975.

Lay, T., J. Ritsema, C. J. Ammon, and T. Wallace, Rapid source mechanism analysis of the April 29, 1993 Cataract Creek (M_w = 5.3), Northern Arizona earthquake, *Bull. Seismol. Soc. Am., 84*, 451-457, 1994a.

Lay, T., C. J. Ammon, A. A. Velasco, J. Ritsema, T. C. Wallace, and H. J. Patton, Near-real-time seismology: Rapid analysis of earthquake faulting, *GSA Today, 4*, 129, 132-134, 1994b.

Nabelek, J. L, Determination of earthquake source parameters from inversion of body waves, Ph.D. thesis, Mass. Inst. of Technology. Cambridge, 1984.

Nabelek, J. L., and G. Xia, Moment-tensor analysis using regional data: Application to the 25 March, 1993, Scotts Mills, Oregon, earthquake, *Geophys. Res. Lett., 22*, 13-16, 1995.

Nakanishi, I., Y. Hanakago, T. Moriya, and M. Kasahara, Performance test on long-period moment tensor determination for near earthquakes by a sparse local network, *Geophys. Res. Lett., 18*, 223-226, 1991.

Patton, H. J., and G. Zandt, Seismic moment tensors of western United States earthquakes and implications for the tectonic stress field, *J. Geophys. Res., 96*, 18245-18259, 1991.

Ritsema, J. and T. Lay, Rapid source mechanism determination of large (M_w>5) earthquakes in the western United States, *Geophys. Res. Lett., 20*, 1611-1614, 1993.

Romanowicz, B. A., Moment tensor inversion of long period Rayleigh waves: A new approach, *J. Geophys. Res., 87*, 5395-5407, 1982.

Romanowicz, B., D. Dreger, M. Pasyanos, and R. Uhrhammer, Monitoring of strain release in central and northern California using broadband data, *Geophys. Res. Lett., 20*, 1643-1646, 1993.

Romanowicz, B., D. Neuhauser, B. Bogaert, and D. Oppenheimer, Accessing northern California earthquake data via internet, *Eos Trans. AGU, 75*, 257, 259-260, 1994.

Ruff, L., and H. Kanamori, The rupture process and asperity distribution of three great earthquakes from long-period diffracted *P* waves, *Phys. Earth Planet. Inter., 31*, 202-230, 1983.

Sipkin, S. A., Estimation of earthquake source parameters by the inversion of waveform data: synthetic seismograms, *Phys. Earth Planet. Inter., 30*, 242-259, 1982.

Thio, H.-K., and H. Kanamori, Moment tensor inversion for local earthquakes using surface waves recorded at TERRAscope, *Bull. Seismol. Soc. Am.*, in press 1995.

Uhrhammer, R., Broadband near-field moment tensor inversion, *EOS Trans. AGU., 73*, 1992.

Wald, D. J., D. V. Helmberger, and T. H. Heaton, Rupture model of the 1989 Loma Prieta earthquake from the inversion of strong-motion and broadband teleseismic data, *Bull. Seismol. Soc. Am., 81*, 1540-1572, 1991.

Wallace, T. C., and D. V. Helmberger, Determining source parameters of moderate-size earthquakes from regional waveforms, *Phys. Earth Planet. Inter., 30*, 185-196, 1982.

Walter, W., Source parameters of the June 29, 1992 Little Skull Mountain earthquake from complete regional waveforms at a single station, *Geophys. Res. Lett., 20*, 403-406, 1993.

Zhang, J., and H. Kanamori, Depths of large earthquakes determined from long-period Rayleigh waves, *J. Geophys. Res., 93*, 4850-4868, 1988.

Zhao, L-S., and D. V. Helmberger, Broadband modeling along a regional shield path, Harvard recording of the Saguenay earthquake, *Geophys. J. Int., 105*, 301-312, 1991.

Zhao, L.-S, and D. V. Helmberger, Source retrieval from broadband regional seismograms: Hindu Kush region, *Phys. Earth Planet. Inter., 78*, 69-95, 1993.

Zhao, L.-S., and D. V. Helmberger, Source estimation from broadband regional seismograms, *Bull. Seismol. Soc. Am., 84*, 91-104, 1994.

T. Lay and J. Ritsema, Institute of Tectonics, University of California, Santa Cruz, CA 95064 (e-mail: jeroen@earthsci.uscs.edu)

(Received August 22, 1994; revised January 18, 1995; accepted January 19, 1995.)